

# Spin Photonic Topological Insulator Leaky Wave Antenna By Armchair Arrangement

Sayyed Ahmad Abtahi\*, Mohsen Maddahali<sup>†</sup>, Ahmad Bakhtafrouz<sup>‡</sup>

Department of Electrical and Computer Engineering,

Isfahan University of Technology,

Isfahan 84156-83111, Iran

\*abtahi.a@ec.iut.ac.ir; <sup>†</sup>maddahali@iut.ac.ir ; <sup>‡</sup>bakhtafrouz@iut.ac.ir

**Abstract**—A leaky wave antenna based on spin photonic topological insulators has been developed, featuring a hexagonal unit cell arranged in an armchair configuration. This configuration offers advantages over the zigzag arrangement, particularly with its wider leaky region and more suitable pattern. While the proposed antenna is a uniform leaky wave antenna, it is capable of radiating in both backward and forward directions. Notably, the transition through the broadside in the scanning range does not result in a significant drop in performance, despite the presence of an open stop band. This characteristic is unique among leaky wave antennas, to the best of our knowledge.

**Index Terms**—Topological insulators, Metasurface, Leaky wave antenna, Armchair arrangement

## I. INTRODUCTION

Photonic topological insulators (PTIs) newly advent to use in guiding-wave and antenna applications, which are robust to scattering from manufacturing defects and sharp turns [1]. One of PTI types is spin PTIs, which are reciprocal and realized by spin-degenerate metamaterials [2].

The spin PTI metasurfaces are introduced using a complementary hexagonal unit cell, as illustrated in Fig.1(a). unit cell exhibits fourfold degeneracy at the K/K' symmetry point in its irreducible Brillouin zone (IRBZ). By bringing together the complementary parts, the strong effective magnetoelectric coupling opens a nontrivial band gap at the K/K' points. The proposed topological structure was created by combining the unit cell with its flipped version to form the edge mode at the interface. The unidirectional propagation of wave line through the interface of two parts of the structure is illustrated in zigzag and armchair configurations.

The investigation of a leaky wave antenna utilizing a zigzag arrangement, as explored in [3], highlights several critical issues. These include a narrow bandwidth, restricted backward radiation scanning, coupling between radiating elements, and an inadequate radiation pattern (see Fig.1(b)).

A proven solution to these issues is transforming the unit cell from a hexagonal configuration to a 30-degree rhombic shape. This change facilitates straight-line propagation, effectively minimizing coupling between radiating elements [4]. While the advantages of utilizing 30-degree rhombic cells are significant, it is important to note that they do experience limitations when scanning in the backward direction.

This paper establishes that adopting an armchair arrangement, rather than a zigzag counterpart, effectively mitigates

the identified issues and enables backward-to-forward beam scanning.

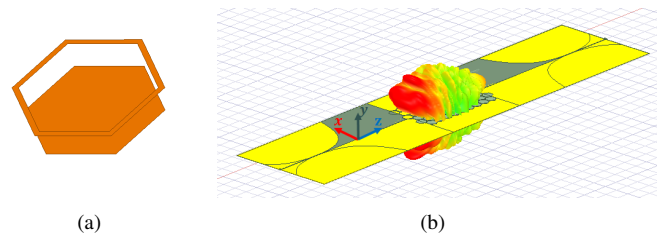


Fig. 1. (a) proposed hexagonal unit cell for topological metasurface in [5]. (b) An example of leaky wave antenna by zigzag arrangement [4]

## II. CHANGING THE ARRANGEMENT

The concept of utilizing the armchair arrangement as a leaky wave antenna derives directly from the trapezoidal serpent line microstrip used in antenna applications [6]. As illustrated in Fig.2, there is a clear analogy between these two structures. In order to compare zigzag and armchair configurations, the dimensions were chosen to match those in [3], featuring a period length of 7 mm and a border width of 0.25 mm. The substrate utilized is a Rogers/Duroid 5880 that has a thickness of 0.127 mm, with a permittivity of 2.2 and a tangent loss factor of 0.0009.

In the initial step, the dispersion diagram for one ribbon from both arrangements is calculated using Ansys HFSS, as

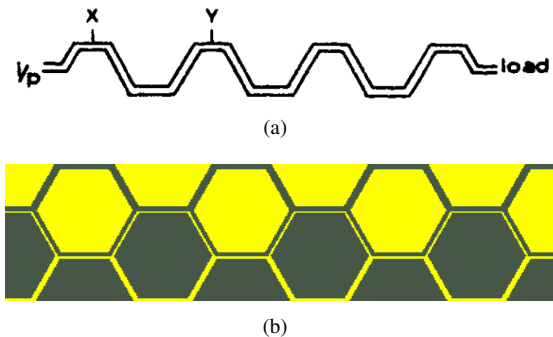


Fig. 2. (a) The trapezoidal serpent line by microstrip [6] (b) hexagonal unit cell of [5] in armchair arrangement.

shown in Fig.3. The primary differences are the alteration in group velocity with increasing frequency and the location of the light line in both diagrams. The group velocity transitions from positive to negative in the zigzag arrangement, whereas it behaves oppositely in the armchair configuration. In Fig.3(a), the position of the light line divides the edge mode region into slow and fast wave domains. In contrast, for the armchair arrangement, all edge modes are located entirely within the fast wave domain. The armchair structure radiates across all edge mode bandwidths, while the zigzag structure starts radiating around 17 GHz. The presence of a bandgap in Fig.3(b) is not a new phenomenon [7]. However, the narrow bandgap in Fig.3(a) arises due to the inclusion of loss in the substrate, which undermines the assumption of electromagnetic duality.

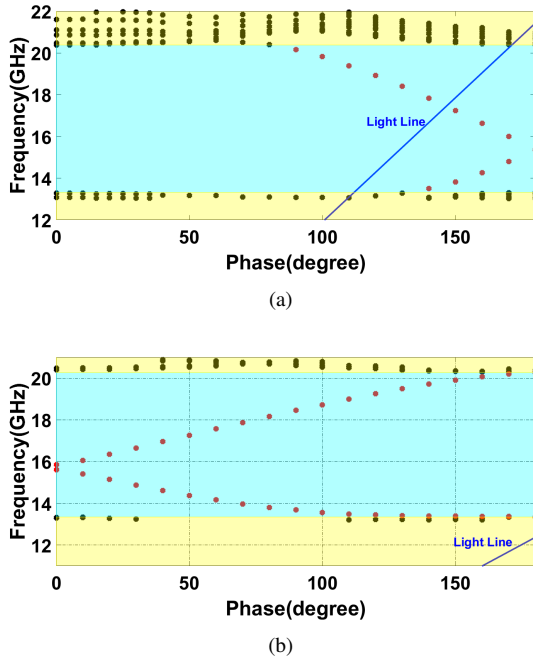


Fig. 3. The dispersion diagram for a single ribbon of the structure is shown, highlighting both the zigzag arrangement ((a)) and the armchair arrangement ((b)). The yellow region, marked with black dots, represents the bulk modes, while the cyan region, indicated with red dots, represents the edge modes.

### III. ANTENNA STRUCTURE

The antipodal slot line (ASL) excitation method was introduced to integrate classical line to topological structure in [8]. However, this method can lead to coupling between the ASL and topological structures arranged in a zigzag configuration. As a result, the armchair arrangement is positioned between two peripheral zigzag structures (see Fig. 4).

Fig.5 illustrates the antenna's return and insertion loss, which corresponds with the dispersion diagrams shown in Fig.3. The bandwidth of exclusive radiation from the armchair section is highlighted in yellow. While in the green frequency interval, both zigzag and armchair configurations emit radiation. The cyan regions represent the gaps in the edge modes, where the return loss increases.

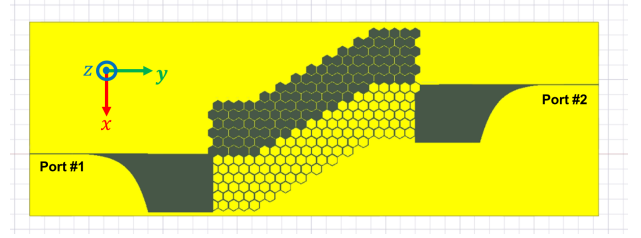


Fig. 4. The antenna configuration by sandwiching the armchair arrangement between two zigzag counterparts and excitation with ASL.

The yellow and green regions are divided into four intervals, and the behavior of the structure changes in each with respect to whether it is right-handed or left-handed.

In domain number ①, the armchair section is left-handed, while the zigzag section is right-handed. In domain number ②, both the armchair and zigzag sections are left-handed. In domain number ③, the armchair section is right-handed, and the zigzag section is left-handed. In domain number ④, the behavior is similar to that of domain ③, but the zigzag section operates in the fast wave regime.

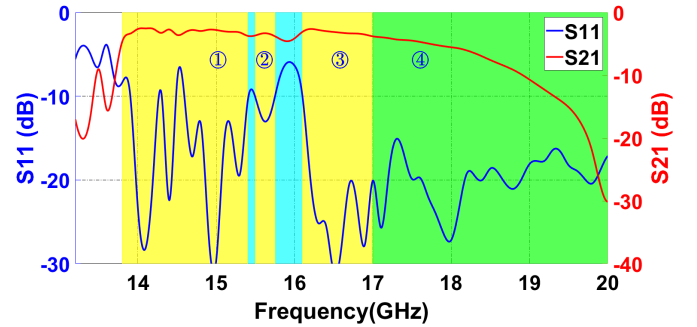


Fig. 5. The Scattering parameters of the proposed antenna. The yellow areas represent the frequencies at which only the armchair portion of the antenna structure radiates. In the green area, both the armchair and zigzag parts radiate simultaneously. The cyan regions indicate the gap in the edge modes, where the return loss increases.

The realized gain pattern at 15.8 GHz, where radiation occurs in a broadside direction, is illustrated in Fig.6. The comparison between the patterns of the zigzag arrangement (Fig.1(b)) and the armchair arrangement indicates that the armchair structure is more suitable than the zigzag one. However, as shown in Fig.5, in the green area where radiation from the zigzag section of the structure occurs, the insertion loss declines rapidly. This qualitatively indicates that the leakage factor of the zigzag structure is higher than that of the armchair structure. As a result of this weaker attenuation, the radiation does not experience a sudden drop in the open stopband regions.

The scan limit of the structure is shown in Fig.7 highlighted in the yellow region of Fig.5, where the armchair section radiates exclusively. Scanning begins at  $-24^\circ$  at 13.8 GHz and, by crossing the broadside, reaches  $12^\circ$  at 17 GHz.

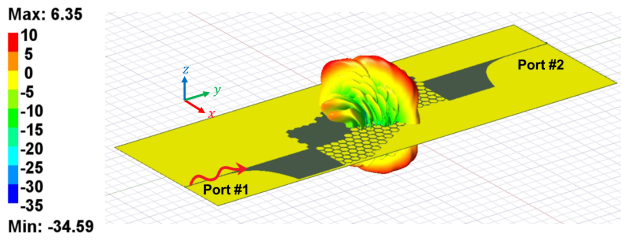


Fig. 6. The realized gain of the antenna in 3D display at 15.8 GHz, where it radiates in broadside and is excited by port 1.

The realized gain in the open stopband at 15.8 GHz is less than -3 dB compared to the values at the ends of the scanning limit. To the best of our knowledge, this unusual phenomenon does not occur in other leaky wave antennas. The 36-degree scan at both the top and bottom of the antenna exceeds the findings reported in [4] and is equal to those in [3], even while crossing the broadside.

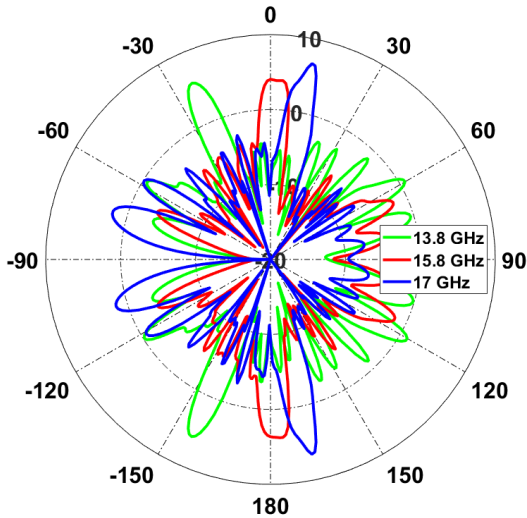


Fig. 7. The realized gain of the antenna at the frequencies of 13.8 GHz, 15.8 GHz, and 17 GHz depicts the structure's scan limit.

#### IV. CONCLUSION

A leaky wave antenna based on spin photonic topological insulators (PTIs) is proposed. It is designed using a hexagonal complementary unit cell arranged in an armchair configuration. This antenna pattern is more practical than its zigzag counterpart. It has a scan range of 36 degrees within a 3.2 GHz bandwidth. Notably, the antenna maintains performance across the broadside without a sharp drop, despite the presence of an open stopband.

#### REFERENCES

[1] T. Ozawa, H. M. Price, A. Amo, N. Goldman, M. Hafezi, L. Lu, M. C. Rechtsman, D. Schuster, J. Simon, O. Zilberberg *et al.*, "Topological photonics," *Reviews of Modern Physics*, vol. 91, no. 1, p. 015006, 2019.

[2] A. B. Khanikaev, S. Hossein Mousavi, W.-K. Tse, M. Kargarian, A. H. MacDonald, and G. Shvets, "Photonic topological insulators," *Nature materials*, vol. 12, no. 3, pp. 233–239, 2013.

[3] S. Singh, D. Bisharat, and D. Sievenpiper, "Topological antennas: Aperture radiators, leaky-wave surfaces, and orbital angular momentum beam generation," *Journal of Applied Physics*, vol. 130, no. 2, p. 023101, 2021.

[4] S. Ahmad Abtahi, M. Maddahali, and A. Bakhtafrouz, "Realizable leaky wave antenna based on spin photonic topological insulators," *IEEE Access*, vol. 12, pp. 152 850–152 859, 2024.

[5] D. J. Bisharat and D. F. Sievenpiper, "Electromagnetic-dual metasurfaces for topological states along a 1d interface," *Laser & Photonics Reviews*, vol. 13, no. 10, p. 1900126, 2019.

[6] J. R. James, P. S. Hall, and C. Wood, *Microstrip antenna: theory and design*. Iet, 1986, vol. 12.

[7] A. H. Castro Neto, F. Guinea, N. M. Peres, K. S. Novoselov, and A. K. Geim, "The electronic properties of graphene," *Reviews of modern physics*, vol. 81, no. 1, pp. 109–162, 2009.

[8] R. J. Davis, D. J. Bisharat, and D. F. Sievenpiper, "Classical-to-topological transmission line couplers," *Applied Physics Letters*, vol. 118, no. 13, p. 131102, 2021.